

Quantum Conductance in Semimetallic Bismuth Nanocontacts

J.G. Rodrigo, A. García-Martín[†], J.J. Sáenz and S.Vieira
Instituto Universitario de Ciencia de Materiales “Nicolás Cabrera”
and
Laboratorio de Bajas Temperaturas,
Departamento de Física de la Materia Condensada,
Universidad Autónoma de Madrid, 28049 Madrid, Spain

Electronic transport properties of bismuth nanocontacts are analyzed by means of a low temperature scanning tunneling microscope. The subquantum steps observed in the conductance versus elongation curves give evidence of atomic rearrangements in the contact. The underlying quantum nature of the conductance reveals itself through peaks in the conductance histograms. The shape of the conductance curves at 77 K is well described by a simple gliding mechanism for the contact evolution during elongation. The strikingly different behaviour at 4 K suggests a charge carrier transition from light to heavy ones as the contact cross section becomes sufficiently small.

PACS numbers: 61.16.Ch, 73.50.-h, 73.23.Ad, 73.20.Dx

In the last few years, several techniques have been extensively used to study the conductance of nanometer-scale contacts with variable cross sections [1–4]. Most of the previous works have been focused on metallic contacts, for which the Fermi wavelength λ_F is very close to the dimensions of the atom. The elongation of the contact produces discrete changes in the cross section (i.e. in the number of atoms) resulting in abrupt jumps in the experimental $G - Z$ curves (conductance vs. elongation of the contact). These jumps are of the order of the conductance quantum $G_0 = 2e^2/h$ since the addition of one atom to the contact is accompanied by the opening of one or few conduction channels depending on the metal [5]. This interplay between electronic and mechanical properties in metallic contacts [6,7] makes it difficult to observe “pure” quantum effects on the conductance.

On the other hand, semimetallic nanocontacts could provide a unique laboratory to investigate quantum conductance phenomena in three-dimensional wires. The high value of λ_F in these systems requires large contact areas in order to have total transmissions of the order of a conductance quantum. As a consequence, it will be possible to distinguish between atomic rearrangements and quantum effects. However, earlier experimental results did not clarify the situation. The first experiments [8] on semimetallic Sb contacts showed several sharp jumps in the $G - Z$ curves for conductances much lower than the quantum unit, proving that, indeed, many atoms are necessary in order to obtain a value of the conductance equal to G_0 . Nevertheless the conductance quantization features were absent probably due to a strong backscattering [8] or to the large angular opening [9] of the contact. More recently, conductance experiments [10] on Bi nanowires at 4K presented a very different behaviour showing, in some situations, long conductance plateaus close to integer multiples of G_0 . After statistical averaging of many consecutive curves, the histogram of conductance values showed the existence of two peaks close

to G_0 and $2G_0$. However, the shape of the histogram exhibited strong deviations from those reported in metallic contacts.

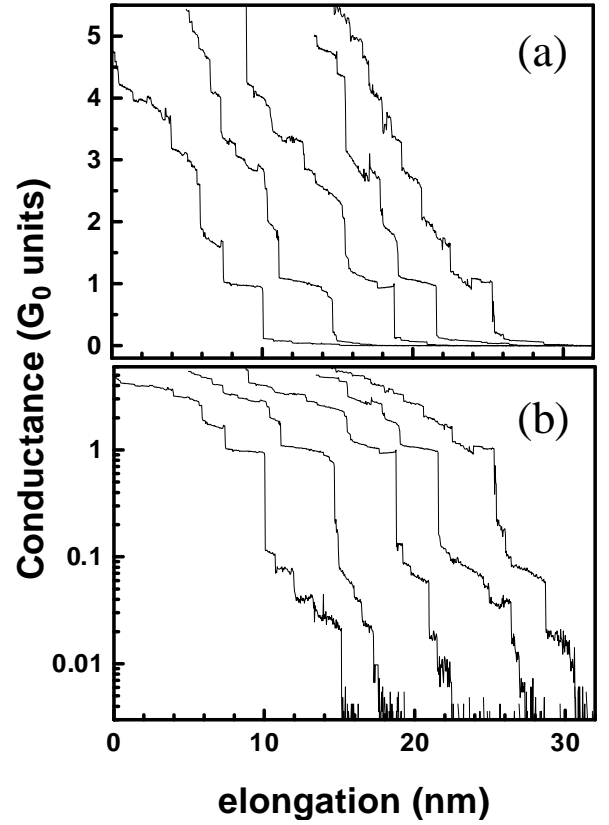


FIG. 1. Typical $G - Z$ curves corresponding to elongation-contraction cycles measured at 77 K: (a) linear scale, (b) logarithmic scale. Curves are shifted horizontally for clarity.

In order to shine some light on the physics of semimetallic contacts, we have performed scanning tun-

neling microscopy (STM) experiments on Bi nanocontacts at different temperatures. First, we analyze in detail the opening of the first conduction channel, which is a particularly difficult task in metallic contacts, where the transition from the tunneling regime into contact is governed by the well known jump-to-contact phenomenon [11]. The peculiar electronic structure of bismuth [12,13] enables a selection of the carrier type, depending on the dimensions of the contact and temperature [14]. This effect will be studied at 77K and 4.2K for contacts with typical conductances in the range $0 < G < 2G_0$. The co-existence of conductance quantization effects and atomic rearrangements will be studied through conductance histograms of the $G - Z$ curves. Due to the fact that even for low conductance values many atoms will be forming the contact, the evolution of the $G - Z$ curves will be analyzed in terms of a simple gliding mechanism that describes the variation of the contact shape during the elongation process.

The experiments have been performed using a high stability scanning tunneling microscope (STM) which can be operated over the range 2 K - 300 K inside a ^4He cryostat. We have used high-purity (99.999%) polycrystalline bismuth, cut from a rod, for both STM tip and sample. Prior to the measurements the surfaces were cut and scratched. At a given location on the sample, the tip is crashed forcibly and repeatedly into the substrate, causing extended plastic deformations that lead to a connective neck between tip and sample. Different neck geometries can be obtained by varying the indentation depth [7]. In Fig. 1 (Fig. 2) we show typical $G - Z$ curves corresponding to a series of consecutive elongation cycles measured at 77K (4K). Continuous cycles of elongation-contraction of a neck lead to situations in which the $G - Z$ curve presents clear steps over the entire conductance range (typically from 0 to $10 G_0$). Although the curves are not reproducible they show a very similar shape. Typically, the length of the steps varies between 0.2 and 1 nm, depending on the initial conditions of the elongation-contraction cycle (i.e., the neck) [15]. These values are close to the lattice parameter of Bi (0.475nm). At 77 K the conductance steps have a small positive slope without specific structure. However, at 4K the first plateaus with $G \gtrsim G_0$ usually show smooth curved shapes which resemble those observed for metallic Al contacts [16,17]. Moreover, the conductance discontinuities ΔG are closer to G_0 , suggesting that at 4K bismuth exhibits a metallic-like behaviour, with a smaller λ_F . Therefore, only a few atoms are involved in the contact. Distortions of the lattice parameter at the contact, together with the peculiar band structure of bismuth, are responsible of the curved plateaus obtained at 4 K.

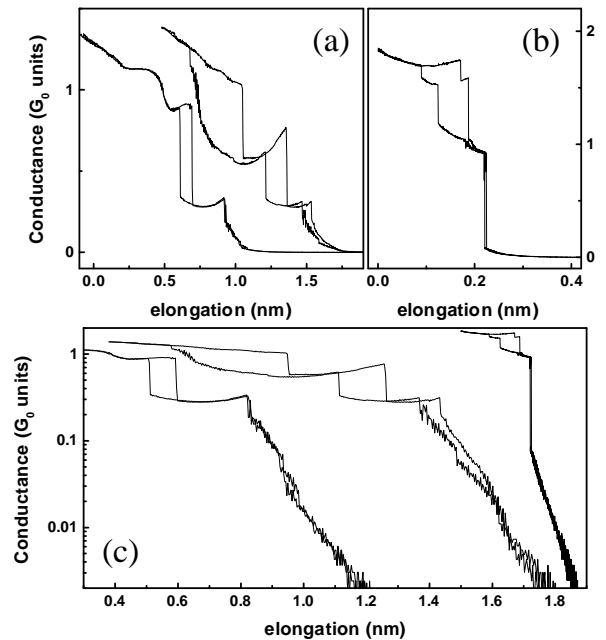


FIG. 2. Typical elongation-contraction cycles measured at 4 K: (a) and (b) linear scale, (c) logarithmic scale. The cycles shown in (a) (the two cycles on the left in (c)) present the sub-quantum conductance jumps and steps. The cycle in (b) (the rightmost one in (c)) shows a contact breaking process. Curves are shifted horizontally for clarity.

As expected for a semimetallic contact, in the subquantum conductance regime the $G - Z$ curves show clear steps at both temperatures (see Figs. 1 and 2). Except for the small jump discontinuities (caused by rearrangements of the atoms and thus reflecting mechanical contact), G decreases exponentially as a function of Z like in a vacuum tunneling process, but with an effective tunneling barrier that strongly depends on temperature (see Figs. 1b and 2b). While at 77K the effective barriers are typically of the order of 10meV, those obtained at 4K are close to 1eV. When the contact finally breaks, the conductance is usually so small that, due to limitations of our current experimental setup, we are not able to observe the transition from “contact” tunneling to actual vacuum tunneling. All these facts indicate that, even at these very small values of the conductance, tip and sample are still in mechanical contact. At 4K there are some situations (see Fig. 2(b), and the curve on the right hand side in Fig. 2(c)), in which the contact breaks before the subquantum conductance regime. In those cases, the conductance does not display subquantum steps and decreases exponentially as a function elongation, where the effective tunneling barrier $\phi \approx 4\text{eV}$ is very close to the expected bismuth work function.

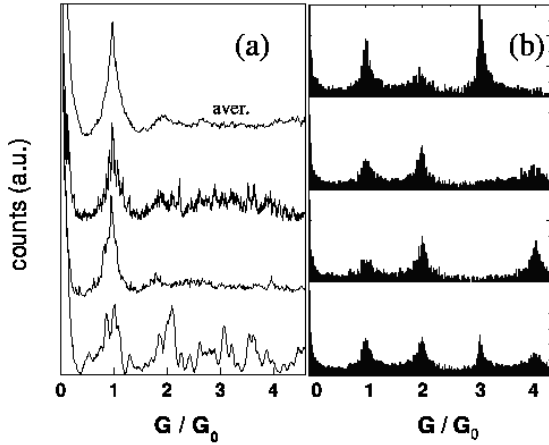


FIG. 3. Histograms of the conductance values obtained for different necks at 77 K. (a) Experimental results from 200 $G - Z$ curves. The top histogram is an average of histograms corresponding to 10 different necks. (b) Histograms obtained from the simulation of different initial necks.

A detailed theoretical description of the electrical properties of the contact during elongation is a very difficult task. The effective mass of the charge carriers in Bi varies over a wide range from $m^* \approx 0.002m_0$ for light electrons to $m^* \approx m_0$ for heavy electrons (m_0 is the electron mass) and depends on the crystal orientation [12,13]. Moreover, the peculiar electronic properties of bismuth (semimetallic character, band filling, Fermi surface, ...) may also vary with lattice deformations due to the extreme uniaxial strains occurring in small contacts [17] during the elongation-compression processes. The apparent metallic behaviour at 4K can be qualitatively understood in terms of quantum finite size effects [18,14]: as the contact radius R decreases the quantized transversal momentum $k_n \propto 1/R$ increases. This leads to a shift in the subband energy position [14], $E_n \approx \hbar^2/(2m^*)k_n^2$ (larger for light carriers) and the gap between light and heavy electrons increases. At low temperatures, there is a transition from light carriers at large cross sections to predominantly heavy electron transport for small cross sections where the light electron states become empty. This qualitative discussion is fully consistent with the analysis of the tunneling regime in mechanical contact ($G < G_0$): The effective barriers in mechanical contact are related to the electron confinement in the constriction. In a free electron picture, the longitudinal momentum of each transversal mode or channel n is given by $k_{zn} = \sqrt{K_F^2 - k_n^2}$ (with $K_F = 2\pi/\lambda_F$) such that to each channel n corresponds a 1D effective potential barrier in the longitudinal direction [9,19]. The modes with $k_n > K_F = (2\pi/\lambda_F)$ are evanescent or tunneling modes. When $R \lesssim \lambda_F$ there is no room even for a single channel and the conductance is dominated by electron tunneling through the first channel with $k_{z1} \approx ik_n \approx i\pi/R$. Assuming that the constriction length increases linearly with the elongation Z

we will roughly have $G \propto \exp(-\frac{\pi}{R}Z)$. Therefore, in the tunneling regime (before the contact breaks), the slope of $\ln G$ as a function of Z gives the order of magnitude of the lateral size of the constriction. Our results then suggest, that, at high temperatures, subquantum steps are related to structural changes of constrictions involving hundreds of atoms (R is a few nanometers). Since the Fermi wavelength is larger or of the order of R , it would also be of the order of a few nanometers. In contrast, at low temperatures subquantum conductance steps can be associated with changes in constrictions consisting of a few atoms (R is now a few Å). This would imply λ_F to be one order of magnitude smaller than before. As mentioned above, this qualitative discussion is fully consistent with the behaviour of the $G - Z$ curves in the range of a few conductance quanta.

The observation of subquantum steps in the $G - Z$ curves provides evidence of atomic rearrangements in the contact. Since these curves are not exactly reproducible from cycle to cycle, conductance quantization effects are difficult to observe from a single elongation curve. After the formation of a given neck, a histogram is obtained from 200 consecutive $G - Z$ curves. In fig. 3(a) we present a set of histograms obtained from different initial necks. As it can be seen, the histograms present peaks close to integer multiples of G_0 which, in contrast with metallic contacts, can be unambiguously associated with conductance quantization effects. In general, we observe that the histogram shape (peak height, number of peaks, ...) changes from neck to neck [15]. This behaviour is clearly different than that observed in some metals (e.g. gold nanocontacts [4]). After averaging over 10 different necks, the resulting histogram (uppermost in Fig. 3a) still shows clear peaks at 1 and 2 conductance quanta which now resemble those of metallic contacts. However, in semimetallic contacts a variation of a few quanta in the conductance requires cross sections much larger than those in metallic ones. Therefore, the mechanical evolution in these systems is expected to be rather different than in metals. For cross sections larger than a few nanometers, yielding occurs as a consequence of collective shear events [20,21]. A qualitative picture of the mechanical evolution can be obtained from a simple model system. We shall restrict ourselves to the tensile loading regime during the elongation of the neck. Suppose that the initial constriction is represented by a cylinder of radius R_0 and consider the deformation process sketched in the inset in Fig. 4(b). The contact is assumed to glide along a symmetry plane that forms an angle θ with respect to the cylinder axis. The maximum elongation Z_{max} before the contact breaks down, is given by $Z_{max} = 2R_0/\tan(\theta)$. For a finite elongation $\tilde{Z} = Z/Z_{max}$, the contact area A shrinks according to (see inset Fig. 4(b)):

$$A(\tilde{Z}) = 2R_0^2 \left(\arccos(\tilde{Z}) - \tilde{Z}\sqrt{1 - \tilde{Z}^2} \right). \quad (1)$$

Interestingly, the contact loses its axial symmetry and the narrowest section of the contact resembles an elliptical cross section (Fig. 4(b)) with an axis aspect ratio $\eta(\tilde{Z}) \approx \pi R_0^2(1 - \tilde{Z})^2/A$. An estimation of the transmission coefficients T_{nm} as a function contact elongation can be obtained from a simple model based on the saddle-point-contact model [22,23]. The geometry of our contact resembles the wide-narrow-wide geometry with ‘elliptical’ cross section discussed in Ref. [23]. Therefore, T_{nm} can be approximated by:

$$T_{nm} = \left[1 + \exp \left(\frac{-2\pi(\sqrt{\pi A} - \epsilon_{nm})}{\tan \alpha} \right) \right]^{-1} \quad (2)$$

where $\epsilon_{nm} = (n + 1/2)/\sqrt{\eta} + \sqrt{\eta}(m + 1/2)$ (all the lengths are in units of λ_F), and $\tan \alpha = \sqrt{(A(0) - A(\tilde{Z}))/\pi/Z_{max}}$ defines the effective “opening angle” [9] of the constriction. The conductance curves are obtained from the Landauer formula, $G = \sum_{nm} T_{nm}$.

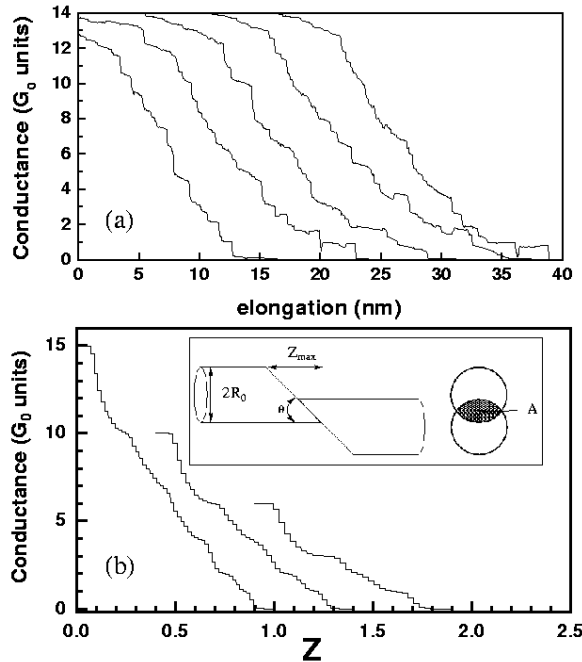


FIG. 4. (a) Experimental $G - Z$ curves at 77 K. (b) Simulated $G - Z$ curves according to the model described in the text (different initial conditions). Inset: sketch of the deformation process.

Typical $G - Z$ curves obtained by this simple model for $\theta = 50^\circ$ are shown in Fig. 4 together with some experimental results at 77K. In order to mimic the stepped structure, the cross section is assumed to be constant within a lattice parameter of Bi. Experimentally the conductance changes from $\approx 10G_0$ to G_0 after an elongation of the contact of the order of 15 nm. Within our model this fixes the Fermi wavelength to be in the nanometer scale, in agreement with the analysis of the subquantum

regime. For small Z , i.e. for small opening angles, there is almost no scattering (the T_{nm} 's are 0 or 1). Therefore, the conductance is simply given by the number of propagating channels in the initial contact N_0 , i.e., those nm channels having $\epsilon_{nm} < \sqrt{\pi A}$. As the elongation proceeds an interesting interplay between the narrowing of the constriction and the change of degeneracy of transversal modes can be observed. For $\tilde{Z} = 0$ the contact has cylindrical symmetry and the transversal levels exhibit the well known degeneracy of a parabolic confining potential. Depending on the initial contact cross section, the conductance is then given by 1, 3, 6, 10, $\dots G_0$. As \tilde{Z} increases, the cross section decreases and, at the same time, the degree of anisotropy $\eta(\tilde{Z})$ also varies, removing the mentioned degeneracy. The conductance behaviour along the elongation path depends critically on the initial conditions of the contact. The theoretical histograms (Fig. 3(b)) strongly depend on the initial cross section and exhibit an overall shape that is very similar to the experimental one.

In summary, the above experiments provide direct experimental evidence for the presence of conductance quantization in three-dimensional nanocontacts, as well as an experimental exploration of the conductance regime prior to the opening of the first quantum channel. Our results for moderate-sized contacts are well described by a simple model of contact evolution during an elongation process that is based on a gliding mechanism. In agreement with magnetotransport measurements, the differences observed between 77K and 4K curves for $G \lesssim G_0$ are consistent with a transition from light to heavy electrons at the Fermi level when the contact cross section becomes sufficiently small. Finally, we consider that our work opens a new way to perform experiments on quantum coherence phenomena in atomic scale contacts that up to now were doable with semiconducting heterostructures only.

This research was supported by the DGICYT (Spain) through grants BFM2000-1470-C02-02, PB98-0464 and PB97-0068.

[†] Present address: Institut für Theorie der Kondensierten Materie, Universität Karlsruhe, P.O. Box 6980, 76128 Karlsruhe, Germany

- [1] C.J. Muller, J.M. van Ruitenbeek and L.J. de Jongh, Phys. Rev. Lett. **69**, 140 (1992); J.M. Krasns *et al.*, Nature **375**, 767 (1995).
- [2] N. Agraït, J.G. Rodrigo and S. Vieira, Phys. Rev. B **47**, 12345 (1993); J.I. Pascual *et al.*, Phys. Rev. Lett. **71**, 1852 (1993); L. Olesen *et al.*, Phys. Rev. Lett. **72**, 2251 (1994).
- [3] J.L. Costa-Krämer, N. García and P. García-Mochales

- and P.A. Serena, Surf. Sci. Lett. **342**, L1144 (1995).
- [4] P.A. Serena and N. García (eds.), “*Nanowires*”, NATO-ASI Series E: Appl. Sci. **340** (Kluwer, Dordrecht, 1997); J.M. van Ruitenbeek in “*Mesoscopic Electron Transport*”, ed. by L.L. Shon, L.P. Kouwenhoven and G. Schön, NATO-ASI Series E: Appl. Sci. **345** (Kluwer, Dordrecht, 1997) p549-579.
 - [5] E. Scheer *et al.*, Phys. Rev. Lett. **78**, 3535 (1997); Nature **394**, 154 (1998).
 - [6] U. Landman, W.D. Luedtke, N.A. Burnham and R.J. Colton, Science **248**, 454 (1990); T.N. Todorov and A.P. Sutton, Phys. Rev. Lett. **70**, 2138 (1993); J.A. Torres and J.J. Sáenz, Phys. Rev. Lett. **77**, 2245 (1996).
 - [7] N. Agraït *et al.*, Thin Solid Films **253**, 199, (1994); Phys. Rev. Lett. **74**, 3995 (1995); G. Rubio, N. Agraït and S. Vieira, Phys. Rev. Lett. **76**, 2302 (1996); C. Untiedt, G. Rubio, S. Vieira and N. Agraït, Phys. Rev. B **56**, 2154 (1997).
 - [8] J. M. Krans, and J. M. van Ruitenbeek, Phys. Rev. B **50**, 17659 (1994).
 - [9] J.A.Torres, J.I. Pascual and J.J. Sáenz, Phys. Rev. B **49**, 16581 (1994).
 - [10] J.L. Costa-Krämer, N. García and H. Olin, Phys. Rev. Lett. **78**, 4990 (1997).
 - [11] J.K. Gimzewski and R. Möller, Phys. Rev. B **36**, 1284 (1987).
 - [12] S. Golin, Phys. Rev. **166**, 643 (1968); R.D. Brown, R.L. Hartman and S.H. Koenig, Phys. Rev. **172**, 598 (1968).
 - [13] C.R. Ast and H. Hoechst, Phys. Rev. Lett. **87**, 177602 (2001)
 - [14] Z. Zhang, X. Sun, M.S. Dresselhaus and J.Y. Ying, Appl. Phys. Lett. **73**, 1589 (1998).
 - [15] At 4K, even for apparently similar initial conditions, the $G - Z$ curves may differ considerably between each other. Sometimes the step lengths could be extremelly large compared with the lattice parameter thus leading to spurious peaks in the conductance histograms. Clear peaks close to integer multiples of G_0 could only be obtained from selected curves. An averaged histogram over many different initial necks shows no defined peaks at any conductance value.
 - [16] J. M. Krans *et al.*, Phys. Rev. B **48**, 14721 (1993); J. C. Cuevas *et al.*, Phys. Rev. Lett. **81**, 2990 (1998).
 - [17] D. Sánchez-Portal *et al.*, Phys. Rev. Lett. **79**, 4198 (1997).
 - [18] V.N. Lutsikii, JETP Letters **2**, 391 (1965).
 - [19] M. Brandbyge, K.W. Jacobsen and J.K. Nørskov, Phys. Rev. B **55**, 2637 (1997).
 - [20] A. Stalder and U. Dürig, J. Vac. Sci. Technol. B **14**, 1259 (1996); Appl. Phys. Lett. **68**, 637 (1996).
 - [21] U. Landman, W.D. Luedtke, B.E. Salisbury and R.L. Whetten, Phys. Rev. Lett. **77**, 1362 (1996).
 - [22] M. Büttiker, Phys. Rev. B **41**, 7906 (1990); A.G. Scherbakov, E.N. Bogachek and U. Landman, Phys. Rev. B **53**, 4054 (1996).
 - [23] T. López-Ciudad *et al.*, Surf. Sci. Lett **440**, L887 (1999).